Strong Edge Magnetism and Tunable Energy Gaps in Zigzag Graphene Quantum Dots with High Stability

Wei Hu,[1] Yi Huang,[2] Lin Lin,[3, 1] Erjun Kan,[4] Xingxing Li,[5] Chao Yang,[1] and Jinlong Yang[5]

[1]*Computational Research Division, Lawrence Berkeley National Laboratory, Berkeley, California 94720, United States*
[2]*Department of Applied Physics, Xi'an Jiaotong University, Xi'an, Shaanxi 710049, China*
[3]*Department of Mathematics, University of California, Berkeley, California 94720, United States*
[4]*Department of Applied Physics and Institution of Energy and Microstructure,*
Nanjing University of Science and Technology, Nanjing, Jiangsu 210094, China
[5]*Hefei National Laboratory for Physical Sciences at Microscale, Department of Chemical Physics,*
and Synergetic Innovation Center of Quantum Information and Quantum Physics,
University of Science and Technology of China, Hefei, Anhui 230026, China
(Dated: November 1, 2017)

Graphene is a nonmagnetic semimetal and cannot be directly used as electronic or spintronic devices. We demonstrate that graphene quantum dots (GQDs) can exhibit strong edge magnetism and tunable energy gaps due to the presence of localized edge states. By using large-scale first principle density functional theory (DFT) calculations and detailed analysis based on model Hamiltonians, we can show that the zigzag edge states in GQDs become much stronger and more localized as the system size increases. The enhanced edge states induce strong electron-electron interactions along the edges of GQDs, ultimately resulting in a magnetic phase transition from nonmagnetic to intra-edge ferromagnetic and inter-edge antiferromagnetic, when the diameter is larger than 4.5 nm. Our analysis shows that the inter-edge superexchange interaction of antiferromagnetic states between two nearest-neighbor zigzag edges in GQDs is much stronger than that exists between two parallel zigzag edges in GQDs and graphene nanoribbons. Furthermore, such strong and localized edge states also induce GQDs semiconducting with tunable energy gaps, mainly controlled by adjusting the system size. Our results show that the quantum confinement effect, inter-edge superexchange (antiferromagnetic), and intra-edge direct exchange (ferromagnetic) interactions are crucial for the electronic and magnetic properties of zigzag GQDs at the nanoscale.

Engineering techniques that use finite size effect to introduce tunable edge magnetism and energy gap are by far the most promising ways for enabling graphene [1] to be used in electronics and spintronics [2, 3]. Examples of finize sized graphene nanostructures include one-dimensional (1D) graphene nanoribbons (GNRs) [4–13] and zero-dimensional (0D) graphene nanoflakes (GNFs) (also known as graphene quantum dots (GQDs)) [14–25]. It is well known that electronic and magnetic properties [26] of GNRs and GNFs depend strongly on the atomic configuration of their edges, which are of either the armchair (AC) or zigzag (ZZ) types [8].

Edge magnetism has been predicted theoretically [10] and observed experimentally [13] in ZZGNRs. The magnetism results from the antiferromagnetic (AFM) coupling between two parallel ferromagnetic (FM) zigzag edges of ZZGNRs. However, the inter-edge superexchange interaction of such AFM states in ZZGNRs rapidly weakens ($\sim w^{-2}$) as the ribbon-width w increases [12]. Furthermore, the energy gap of GNRs depend on several factors, such as the edge type (armchair or zigzag) and the width of the nanoribbon [8], thus cannot be easily tuned. Such problem does not exist in GNFs due to the quantum confinement effect [27]. The ability to the control GNF energy gap has enabled GNFs to be used in promising applications in electronics [17]. In addition, triangular ZZGNFs are theoretically predicted to have strong edge magnetism even in small systems [28, 29]. Recent experiments [30] have also demon-strated that edge magnetism can be observed in ZZGNFs when the edges are passivated by certain chemical groups. However, triangular ZZGNFs have large formation energy [21] and have not been synthesized experimentally. Interestingly, hexagonal ZZGNFs exhibits significantly improved stability in ambient environment [21]. Theoretically, semi-empirical tight-binding model [31, 32] and first principle density functional theory (DFT) calculations [22–25] for hexagonal ZZGNFs have been performed for small sized systems but found no magnetism (NM). Thus the prospect of finding stable finite sized graphene easily fabricated in experiments that exhibits both strong edge magnetism and tunable energy gap seems dim.

In this letter, we systematically study the electronic and magnetic properties of hexagonal ZZGNFs with the diameters in the range of 2 nm to 12 nm (with up to 3900 atoms). Using first-principles DFT calculations, we find that both strong edge magnetism and tunable energy gap can be realized simultaneously in large ZZGNFs. We demonstrate that spin polarization plays a crucial role as the diameter of a ZZGNF increases beyond 4.5 nm. A spin-unpolarized calculation shows that edge states become increasingly more localized as the size a ZZGNF increases. These edge states form a half-filled pseudo-band and is thus unstable. Adding spin-polarization allows the edge states to spontaneously split into spin-polarized occupied and unoccupied states. This separation results in a magnetic phase transition from an NM phase to a strong inter-edge AFM phase. It also opens a tun-

able band gap that can be easily controlled by quantum confinement effect. These properties make GNFs better candidate materials for nanoelectronics than GNRs [8]. We also confirm that ZZGNFs passivated by different chemical groups all exhibit similar behavior. Such flexibility may facilitate future experimental synthesis of such ZZGNFs.

We use the Kohn-Sham DFT based electronic structure analysis tools implemented in the SIESTA (Spanish Initiative for Electronic Simulations with Thousands of Atoms) [33] software package. We use the generalized gradient approximation of Perdew, Burke, and Ernzerhof (GGA-PBE) [34] exchange correlation functional with collinear spin polarization, and the double zeta plus polarization orbital basis set (DZP) to describe the valence electrons within the framework of a linear combination of numerical atomic orbitals (LCAO) [35]. All atomic coordinates are fully relaxed using the conjugate gradient (CG) algorithm until the energy and force convergence criteria of 10^{-4} eV and 0.02 eV/Å respectively are reached. Due to the large number of atoms contained in hexagonal hydrogen-passivated ZZGNFs ($C_{6n^2}H_{6n}$, $n = 1 \sim 25$), we use the recently developed PEXSI (Pole EXpansion and Selected Inversion) method [36–38] to accelerate the computation.

We demonstrate the importance of spin polarization using $C_{864}H_{72}$ (6 nm) as an example (Figure 1). In spin unpolarized calculations, strong and localized edge states are observed (Figure 1(e)), which induce high electron density on the edges of $C_{864}H_{72}$. Furthermore, such edge states in ZZGNFs becomes much stronger and more localized as the sizes increase [25], which lead to metallic ZZGNFs at the nanoscale [32]. Figure 1(c) plots the projected density of states (PDOS) of the carbon edges of $C_{864}H_{72}$ and shows considerable high density of states (DOS) near the Fermi level. This confirms that $C_{864}H_{72}$ exhibits metallic characteristics in spin unpolarized calculations due to the strong localized edge states [25].

In spin polarized calculations, such half-filled metallic edge states are not stable, and can spontaneously split into two types of occupied and unoccupied states as shown in Figure 1(b) and (d). A magnetic phase transition occurs from the NM phase to a magnetic phase that exhibits intra-edge FM and inter-edge AFM characters as shown in Figure 1(f). This can be interpreted as the Mott-type competition between the kinetic (hopping) energy and the intra-edge (on-site) electron-electron interaction energy with respect to the spin polarized edge states. The minimization of the kinetic energy tends to produce delocalized spin states across all edges, while the minimization of the electron-electron interaction energy tends to penalize simultaneous occupation of the same edge by spin up and spin down electrons. Our calculation indicates that for small system sizes, the kinetic energy dominates, which agrees with previous theoretical prediction of the NM phase for hexagonal ZZGNFs [22–25, 31, 32]. Only as the system size increases, the effective electron-electron interaction energy for the edge states
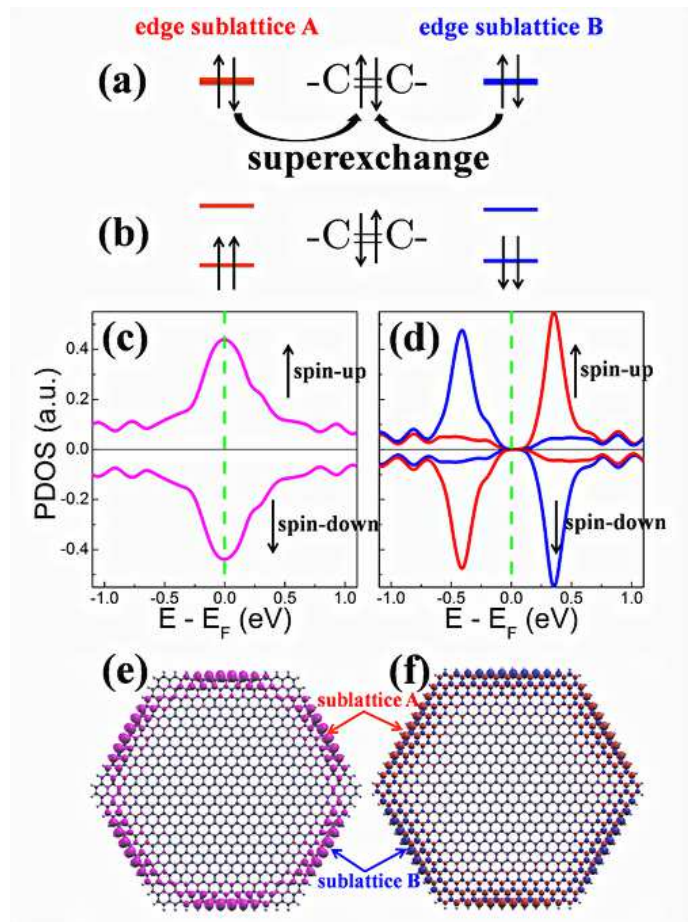

FIG. 1: Electronic structure of edge states in $C_{864}H_{72}$ in two different magnetic phases (NM and AFM), including the schematic illustration of orbital diagram of superexchange interaction of edge states in the (a) NM and (b) AFM phases, projected density of states (PDOS) of edges in the (c) NM and (d) AFM phases, (e) local density of states (LDOS) of Fermi level (pink isosurfaces) in the NM phase and (f) spin density isosurfaces in the AFM phase. The red and blue isosuraces in (f) represent the spin-up and spin-down states, respectively. The red and blue lines in (d) represent the PDOS contributed by sublattice A (spin-up edges) and B (spin-down edges) atoms in graphene, respectively. The fermi level is marked by green dotted lines and set to zero.

starts to dominate and results in the phase transition.

Figure 2(a) shows the variation of relative energy of NM, AFM and FM coupling between different edges in ZZGNFs and ZZGNRs with respect to the system size. Our calculations show the AFM states are much more stable than the NM and FM states in large-scale cases, and a magnetic phase transition (Figure 2(b)) occurs in ZZGNFs as the diameter increases larger than 4.5 nm ($C_{486}H_{54}$) [28]. In detail, the intra-edge direct exchange interactions induce FM states along each zigzag edge (belong to the same sublattice) and the inter-edge superexchange interactions induce AFM states between

two nearest-neighbor edges (belong to different sublattices) through a carbon-carbon double bond (C=C) at the corner in ZZGNFs (Figure 1(a)) at the nanoscale. The local magnetic moment $M_i = |< \hat{n}_{i\uparrow} > - < \hat{n}_{i\downarrow} >|$ ($< \hat{n}_{i\sigma} >$ is spin electron density and $\sigma = \uparrow$ (spin-up) or $\downarrow$ (spin-down)) at the carbon atom i (defined to be the one with the largest magnetic moment in the middle of each zigzag edge in ZZGNFs) increases with the system size, and converges to 0.3 uB when the diameter is larger than than 6 nm ($C_{864}H_{72}$). Furthermore, there is no charge transfer ($< \hat{n}_{i\uparrow} > + < \hat{n}_{i\downarrow} > \approx 4$) between different edge carbon atoms (belong to the same or different sublattices) in ZZGNFs as the system size increases.

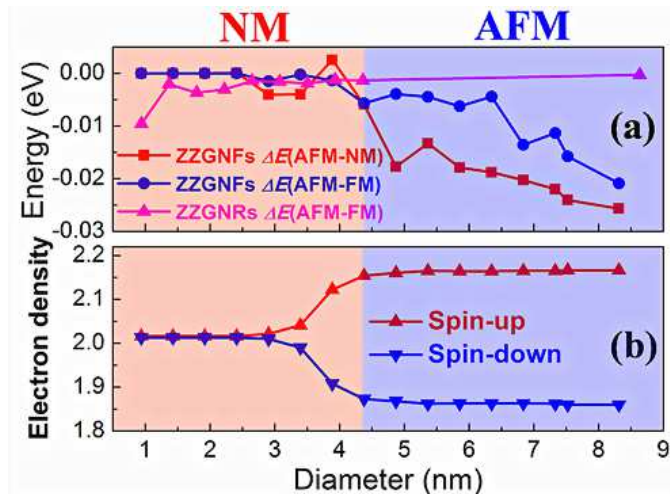FIG. 2: (a) Relative energy per edge atom (ΔE(AFM-NM) and ΔE(AFM-FM)) of NM, AFM and FM coupling between different edges in ZZGNFs and ZZGNRs and (b) spin electron density $< \hat{n}_{i\sigma} >$ ($\sigma = \uparrow$ (spin-up) or $\downarrow$ (spin-down)) at the carbon atom i in the middle of each zigzag edge in AFM ZZGNFs under the variation of the diameter (ZZGNFs) or ribbon-with length (ZZGNRs). The red and blue regions represent the stable NM (ΔE(AFM-NM) ≈ 0) and AFM (ΔE(AFM-NM) < 0) coupling between different edges in ZZGNFs, respectively.

Notice that the intra-edge direct exchange interactions of FM sates along each zigzag edge in ZZGNFs are similar to that in ZZGNRs. However, the inter-edge superexchange interactions of AFM states between two nearest-neighbor edges through a C=C bond at the corner in ZZGNFs (Figure 1(a)) are much stronger than that between two parallel edges through π-electron in ZZGNRs as shown in Figure 2(a), where such AFM coupling weakens rapidly as the ribbon-width increases [12]. Our DFT calculations confirm that the energy difference of AFM and FM coupling between two parallel edges in large-scale 1D ZZGNRs is negligible compared to ZZGNFs reported here.

The enhanced stability of spin-polarized ZZGNFs can be understood by using the Heisenberg model. We consider each FM edge as one site and count the edge magnetic exchange interactions, and the Hamiltonian can be written as

$$\hat{H} = -\sum J_{i,j} \vec{M}_i \vec{M}_j \qquad (1)$$

where $J_{i,j}$ is the exchange parameter between two states i and j, $\vec{M}_i$ and $\vec{M}_j$ are corresponding spin magnetic moments (The details are given in the Supplemental Material). There are four different magnetic states in $C_{864}H_{72}$, three types of antiferromagnetic (AFM, AFM1 and AFM2) and one type of ferromagnetic (FM) coupling at the edges as shown in Figure 3. The total energies of magnetic phases E(AFM), E(AFM1), E(AFM2) and E(FM) can be computed by the DFT calculations, and the the exchange parameters can be evaluated by [39]

$$\begin{aligned}
E(\text{AFM}) &= (6J_1 - 6J_2 + 3J_3)M^2 + E_0 \\
E(\text{AFM1}) &= (2J_1 + 2J_2 - J_3)M^2 + E_0 \\
E(\text{AFM2}) &= (-J_1 + 2J_2 + 3J_3)M^2 + E_0 \\
E(\text{FM}) &= (-6J_1 - 6J_2 - 3J_3)M^2 + E_0
\end{aligned} \qquad (2)$$

where J_1, J_2 and J_3 are ortho-, meta- and para- edge exchange interaction parameters, respectively. M is the spin magnetic moment at each edge. E_0 is nonmagnetic reference total energy. We find that inter-edge exchange strength (J_1 = -0.038351 eV, J_2 = 0.000954 eV and J_3 = 0.001633 eV for $C_{864}H_{72}$) between two nearest-neighbor edges is ten times stronger than that between two parallel edges in ZZGNFs and ZZGNRs. Therefore, ZZGNFs can maintain strong edge magnetism as the system size increases, superior to that in ZZGNRs [7, 12].
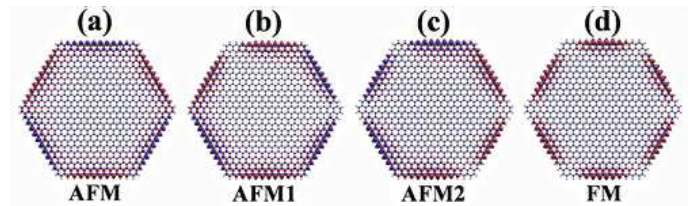

FIG. 3: Spin density isosurfaces of hydrogen-passivated $C_{864}H_{72}$ in four different magnetic states, three types of antiferromagnetic (AFM, AFM1 and AFM2) and one type of ferromagnetic (FM) coupling at the inter edges. The red and blue isosurfaces represent the spin-up and spin-down states, respectively.

We also check the effects of different types of passivating atoms (bare and fluorine) and the shape (nonhexagonal) of ZZGNFs on their electronic and magnetic properties, and find that the results of magnetic phase transition and semiconductor characteristics are similar to that in hexagonal hydrogen-passivated ZZGNFs (The details are given in the Supplemental Material) [40]. Such robustness provides flexibility in terms of the chemical environment of ZZGNFs, and thus may facilitate the synthesis of large scales ZZGNFs with tunable edge magnetism and energy gaps as candidates for electronic and spintronic devices [41].

We remark that the magnetic phase transition and associated with tunable electronic structures, especially energy gaps, can also be observed in the Hubbard model [28]. From our first principle calculations, we find that choosing the parameters $t = 2.5$ eV and $U = 2.1$ eV in the Hubbard model can well reproduce the size-dependent energy gaps (The details are given in the Supplemental Material). Figure 4 plots how the HOMO-LUMO energy gap E_g change with respect to the system size of ZZGNFs and ACGNFs in two different magnetic phases (NM and AFM). Our DFT calculations and mean-field Hubbard model show similar results that the energy gaps E_g of ZZGNFs decrease as the system size increases. In particular, we find that the energy gap of NM ZZGNFs decreases more rapidly with respect to the system size than that in AFM ZZGNFs, due to the presence of edge states whose electron density near the edges of ZZGNFs as shown in Figure 1(e). This observation is consistent with previous results obtained from tight-binding models [31, 32] and DFT calculations [24, 25]. However, AFM semiconducting ZZGNFs show similar scaling behavior of the energy gap to NM ACGNFs at the nanoscale [25]. Therefore, edge states should have little effect on the energy gaps of AFM ZZGNFs and the quantum confinement effect[27] is the only factor to control the energy gaps in ZZGNFs and ACGNFs (Figure 4(a)). In detail, NM ZZGNFs exhibits metallic characters (E_g is smaller than the thermal fluctuation (25 meV) at room temperature) when the diameter is larger than 7 nm ($C_{1350}H_{90}$), but AFM ZZGNFs with the diameter of 12 nm ($C_{3750}H_{150}$) still behaves as a semiconductor with a sizable energy gap $E_g = 0.23$ eV, similar to the case of NM ACGNFs [25].
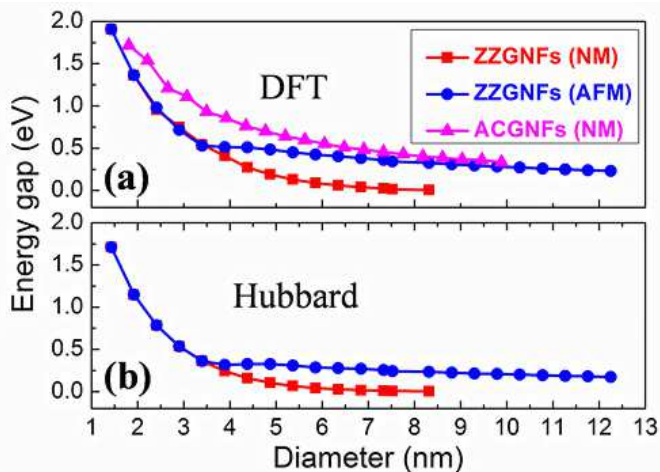

FIG. 4: Energy gap E_g (eV) of ZZGNFs and ACGNFs in two different magnetic phases (NM and AFM) as a function of the diameter size (nm), computed with two different methods, (a) DFT calculations and (b) Hubbard model ($t = 2.5$ eV and $U = 2.1$ eV).

In summary, using large scale first principle calculations, we show that the electronic and magnetic properties of hexagonal zigzag graphene quantum dots (GQDs) can be significantly affected by the system size. We found that the zigzag edge states in GQDs become much stronger and more localized as the system size increases. The presence of these edge states induce strong electron-electron interactions along the edges of GQDs, resulting in a magnetic phase transition from nonmagnetic to intra-edge ferromagnetic and inter-edge antiferromagnetic when the diameter is larger than 4.5 nm. On the other hand, such strong and localized edge states also induce GQDs semiconducting with tunable energy gaps only controlled by adjusting the system size. Therefore, ZZGNFs with strong edge magnetism and tunable energy gaps may be promising candidates and practical electronic and spintronic applications.

[1] K. S. Novoselov, A. K. Geim, S. V. Morozov, D. Jiang, Y. Zhang, S. V. Dubonos, I. V. Grigorieva, and A. A. Firsov, Scinece **306**, 666 (2004).

[2] A. K. Geim and K. S. Novoselov, Nature Mater. **6**, 183 (2007).

[3] A. H. C. Neto, F. Guinea, N. M. R. Peres, K. S. Novoselov, and A. K. Geim, Rev. Mod. Phys. **18**, 109 (2009).

[4] M. Y. Han, B. Özyilmaz, Y. Zhang, and P. Kim, Phys. Rev. Lett. **98**, 206805 (2007).

[5] X. Li, X. Wang, L. Zhang, S. Lee, and H. Dai, Science **319**, 1229 (2008).

[6] X. Jia, M. Hofmann, V. Meunier, B. G. Sumpter, J. Campos-Delgado, J. M. Romo-Herrera, H. Son, Y.-P. Hsieh, A. Reina, J. Kong, et al., Science **323**, 1701 (2009).

[7] Y.-W. Son, M. L. Cohen, and S. G. Louie, Nature **444**, 347 (2006).

[8] Y.-W. Son, M. L. Cohen, and S. G. Louie, Phys. Rev. Lett. **97**, 216803 (2006).

[9] L. Yang, C.-H. Park, Y.-W. Son, M. L. Cohen, and S. G. Louie, Phys. Rev. Lett. **99**, 186801 (2007).

[10] E. Kan, Z. Li, J. Yang, and J. G. Hou, J. Am. Chem. Soc. **130**, 4224 (2008).

[11] M.-Q. Long, L. Tang, D. Wang, L. Wang, and Z. Shuai, J. Am. Chem. Soc. **131**, 17728 (2009).

[12] J. Jung, T. Pereg-Barnea, and A. H. MacDonald, Phys. Rev. Lett. **102**, 227205 (2009).

[13] G. Z. Magda, X. Jin, I. Hagymási, P. Vancsó, Z. Osváth, P. Nemes-Incze, C. Hwang, L. P. Biró, and L. Tapasztó, Nature **514**, 608 (2014).

[14] L. A. Ponomarenko, F. Schedin, M. I. Katsnelson, R. Yang, E. W. Hill, K. S. Novoselov, and A. K. Geim, Science **320**, 356 (2008).

[15] N. G. Shang, P. Papakonstantinou, M. McMullan, M. Chu, A. Stamboulis, A. Potenza, S. S. Dhesi, and H. Marchetto, Adv. Funct. Mater. **18**, 3506 (2008).

[16] A. L. V. de Parga, F. Calleja, B. Borca, M. C. G. Passeggi, J. J. H. Jr., F. Guinea, and R. Miranda, Phys. Rev. Lett. **100**, 056807 (2008).

[17] K. A. Ritter and J. W. Lyding, Nature Mater. **8**, 235 (2009).

[18] A. Kuc, T. Heine, and G. Seifert, Phys. Rev. B **81**, 085430 (2010).

[19] M. Wimmer, A. R. Akhmerov, and F. Guinea, Phys. Rev. B **82**, 045409 (2010).

[20] G. Eda, Y.-Y. Lin, C. Mattevi, H. Yamaguchi, H.-A. Chen, I.-S. Chen, C.-W. Chen, and M. Chhowalla, Adv. Mater. **22**, 505 (2010).

[21] P.-C. Lin, Y.-R. Chen, K.-T. Hsu, T.-N. Lin, K.-L. Tung, J.-L. Shen, , and W.-R. Liu, Phys. Chem. Chem. Phys. **19**, 6338 (2017).

[22] Y. Zhou, Z. Wang, P. Yang, X. Sun, X. Zu, and F. Gao, J. Phys. Chem. C **116**, 5531 (2012).

[23] N. Wohner, P. Lam, and K. Sattler, Carbon **67**, 721 (2014).

[24] S. K. Singh, M. Neek-Amal, and F. M. Peeters, J. Chem. Phys. **140**, 074304 (2014).

[25] W. Hu, L. Lin, C. Yang, and J. Yang, J. Chem. Phys. **141**, 214704 (2014).

[26] O. V. Yazyev, Rep. Prog. Phys. **73**, 056501 (2010).

[27] J. Raty, G. Galli, and T. van Buuren, Phys. Rev. Lett. **90**, 037401 (2003).

[28] J. Fernández-Rossier and J. J. Palacios, Phys. Rev. Lett. **99**, 177204 (2007).

[29] W. L. Wang, S. Meng, and E. Kaxiras, Nano Lett. **8**, 241 (2008).

[30] Y. Sun, Y. Zheng, H. Pan, J. Chen, W. Zhang, L. Fu, K. Zhang, N. Tang, and Y. Du, npj Quantum Materials **2**, 5 (2017).

[31] Z. Z. Zhang, K. Chang, and F. M. Peeters, Phys. Rev. B **77**, 235411 (2008).

[32] A. D. Güçlü, P. Potasz, and P. Hawrylak, Phys. Rev. B **82**, 155445 (2010).

[33] J. M. Soler, E. Artacho, J. D. Gale, A. García, J. Junquera, P. Ordejón, and D. Sánchez-Portal, J. Phys.: Condens. Matter **14**, 2745 (2002).

[34] J. P. Perdew, K. Burke, and M. Ernzerhof, Phys. Rev. Lett. **77**, 3865 (1996).

[35] J. Junquera, O. Paz, D. Sánchez-Portal, and E. Artacho, Phys. Rev. B **64**, 235111 (1996).

[36] L. Lin, J. Lu, L. Ying, R. Car, and W. E, Comm. Math. Sci. **7**, 755 (2009).

[37] L. Lin, M. Chen, C. Yang, and L. He, J. Phys.: Condens. Matter **25**, 295501 (2013).

[38] L. Lin, A. García, G. Huhs, and C. Yang, J. Phys.: Condens. Matter **26**, 305503 (2014).

[39] X. Li, X. Wu, and J. Yang, J. Am. Chem. Soc. **136**, 5664 (2014).

[40] M. Kabir and T. Saha-Dasgupta, Phys. Rev. B **90**, 035403 (2014).

[41] P. Hawrylak, F. Peeters, and K. Ensslin, Phys. Status Solidi RRL **10**, 11 (2016).